Polymer 103 (2016) 397–404

Contents lists available at ScienceDirect

Polymer

journal homepage: www.elsevier.com/locate/polymer

The influence of surface properties on sliding contact temperature and friction for polyetheretherketone (PEEK)

K.A. Laux [a, 1], A. Jean-Fulcrand [b, 1], H.J. Sue [a, **], T. Bremner [c], J.S.S. Wong [b, *]

[a] Department of Mechanical Engineering, Texas A&M University, College Station, TX, USA
[b] Department of Mechanical Engineering, Imperial College London, UK
[c] Hoerbiger Corporation of America, Inc., Houston, TX, USA

ARTICLE INFO

Article history:
Received 3 June 2016
Received in revised form
8 September 2016
Accepted 18 September 2016
Available online 20 September 2016

Keywords:
In situ thermography
Transfer film
Polyetheretherketone
Friction
Polymer tribology

ABSTRACT

Polyetheretherketone (PEEK) polymers are increasingly used in tribological applications. An important aspect of PEEK tribology is the surface temperature reached during sliding. At present, most knowledge of frictional heating in PEEK is based on post-hoc analysis of debris and wear surfaces. In this study, infrared thermography was used to observe the full field temperature map of PEEK against sapphire counterface during ball-on-disc sliding. The measured temperatures matched closely those predicted by flash temperature models. Additionally, friction studies were performed with steel and sapphire counterfaces. It was observed that PEEK debris readily deposited on steel but not on sapphire. The friction studies also indicated a greater adhesive friction response for PEEK against steel compared to PEEK against sapphire. The transfer of PEEK material to the steel surface may elevate the temperature at the sliding interface. Analysis of transfer films on steel suggests that the transferred PEEK was oriented in the direction of sliding. The deposition of debris and formation of oriented films resembled a high temperature drawing process, which was likely to be due to localized frictional heating. The results of this study illustrate the important role transfer films play in determining both the friction and temperature of the PEEK wear interface.

© 2016 The Authors. Published by Elsevier Ltd. This is an open access article under the CC BY license (http://creativecommons.org/licenses/by/4.0/).

1. Introduction

1.1. Frictional heating

When two surfaces are rubbed against each other, frictional heat is generated and temperature at the rubbing interface rises. Depending on test conditions and material properties of the rubbing pair, the interfacial temperature, T_s, can be substantially higher than the stated test temperature. This is particular true when rubbing surfaces are rough. For rough surfaces, the real contact area is often much smaller than the nominal contact area [1–3]. The asperity contact pressures are thus much greater than that predicted by Hertzian contact mechanics. The high local pressure and friction can give rise to very high local temperatures [4].

The actual magnitude of T_s is important for an accurate description of polymer wear phenomena. Polymers are typically good insulators. Thus heat cannot be conducted away easily and T_s can be high enough to soften or even melt the polymer surface. Severe wear associated with melting are likely to be initiated by the buildup of small thermal transients [5]. Many studies have observed rippled and stretched wear features that suggest the rubbing surface was strained when in a rubbery state [6–8]. Analysis of wear debris often shows changes in molecular structures that indicate surface temperatures near melting were reached [9,10]. Ludema and Rhee utilized mass spectroscopy to examine decomposition products during severe polymer wear [11]. The detection of chemical vapors corresponding to melting implied that melting temperatures T_m have been reached at the rubbing interface. Archard determined maximum temperatures for polymer rubbing pairs based on a model for load-controlled friction [12]. He observed that predicted temperatures near the glass transition temperature T_g corresponded with severe wear in Perspex sliding pairs. Ettles suggested that for polymers, a limiting temperature exists based on a thermal softening point [5]. This thermal control model has been supported by empirical observations of polymer friction [5,13,14]. Despite the important role played by temperature in polymer friction and wear, most of the available temperature data are based on post-hoc analysis or inference from analytical or

* Corresponding author.
** Corresponding author.
E-mail addresses: hjsue@tamu.edu (H.J. Sue), j.wong@imperial.ac.uk (J.S.S. Wong).
[1] These authors contribute equally.

http://dx.doi.org/10.1016/j.polymer.2016.09.064
0032-3861/© 2016 The Authors. Published by Elsevier Ltd. This is an open access article under the CC BY license (http://creativecommons.org/licenses/by/4.0/).

numerical models.

The interfacial temperature due to frictional heating can be estimated based on material properties and sliding speeds. The sharp temperature rise at the contact is termed the flash temperature. Models based on a moving heat source [4,12,15–17] have been proposed to describe situations with a variety of Peclet numbers and shapes of heat source [18]. Early work attempted to confirm these models through the use of buried thermocouples, dyes, and temperature sensitive films [18]. However, advances in infrared (IR) thermography have enabled *in situ* studies of frictional heating to be performed with great accuracy. Results can then be directly compared with flash temperature models [19–22].

In situ frictional heating studies of polymers so far have focused largely on rubber and other soft elastomers [19,22–24]. These materials have low elastic moduli. Thus they have large real contact areas and high friction can occur at low pressures and sliding speeds. These test conditions however differ vastly from operational conditions commonly experienced by many engineering polymers. For instance, a thrust washer configuration may operate with a nominal pressure of ~1 MPa and speeds of 4 m/s [25]. In this work, PEEK polymer, a high performance engineering polymer, was studied across a range of pressures and speeds in which frictional heating was believed to become significant. A ball-on-disc geometry was used where the ball was made of PEEK. The resulting contact pressure may be much greater than is typical of pin on flat or thrust washer configurations. During sliding, the surface temperature was monitored.

1.2. PEEK tribology

Polyetheretherketone (PEEK) is a high performance semi-crystalline polymer from the polyaryletherketone (PAEK) family of thermoplastics [26]. PEEK is valued for its solvent resistance as well as high glass transition (T_g ~ 150 °C) and melting (T_m ~ 350 °C) temperatures [26]. These properties have enabled PEEK to be employed in tribological applications where temperatures and corrosive environments would preclude the use of many materials. PEEK has been used in oil and gas exploration [27], biomedical applications [28], and space environments [29] to name a few. Limits on operating conditions are often ascribed to excessive heating that results from friction [30]. To avoid such conditions, it is not uncommon for an upper value of pressure and velocity to be assigned to PEEK-based components [31–35].

A number of authors have focused on PEEK wear behavior [35–38]. Comparisons in terms of friction and wear resistance are often made with polytertrafluoroethylene (PTFE). PTFE on its own suffers from high wear rates [39]. Unfilled PEEK on the other hand has outstanding wear resistance but tends to have high friction coefficients [39,40]. PEEK is thus often filled with PTFE to reduce friction.

PEEK wear resistance is often attributed to an ability to form protective transfer films on harder metallic counterfaces [7,37]. Unlike PTFE that forms transfer films due to its unique banded crystal structure, there is no specific mechanism for PAEK film formation [41]. When PAEK is rubbed against metal, Bahadur suggested that compacted polymer debris becomes physically entrapped between asperities of the countersurface [42]. A polymeric film is eventually formed, and protects the bulk polymer from abrasive wear by covering hard rough asperities.

Many studies have attempted to understand the thermal and tribochemical effects of PEEK wear. Using thermogravimetric analysis (TGA) and differential scanning calorimetry (DSC), Zhang studied the thermal properties of PEEK debris formed under various conditions [43]. It was believed that during wear, chain scission of the diphenyl ether segment occurs and oxidative crosslinks are formed at free radical sites. They had observed changes in the pyrolysis behavior. In addition, the tendency for crystallization is impeded. These results were suggested to be due to the formation of crosslinked branches that restricted segmental mobility. X-ray photoelectron spectroscopy (XPS) was used to further support this hypothesis and found the severity of chain scission is pressure dependent [44]. The thermal properties of PEEK wear debris also indicate that they were formed near melting temperatures [9,43]. According to Bahadur, the chemical activity between fillers and counterface can enhance the tenacity of polymeric transfer films [45–47]. Jacobs showed that for sliding wear of PEEK in aqueous environments, chemically inert diamond-like coating (DLC) or alumina Al_2O_3 counterfaces should be used in place of steel to reduce wear [48,49]. Rebelo de Figueiredo recently used Raman spectroscopy to detect adhesive transfer between neat PEEK and various counterfaces [50]. Low surface roughness and surface energy were believed to minimize the adhesion tendency as well as tribo-oxidative wear [50]. These observations all indicate that wear behavior of PEEK depends strongly on tribochemistry and temperature. However, these theories can be further supported by *in situ* studies.

The overall aim of this work is to understand how frictional heat manifests during sliding of polyetheretherketone (PEEK) polymers against steel and sapphire surfaces. The effect of contact temperature on friction were investigated. This was accomplished by measuring evolutions of friction and temperature in PEEK sliding contacts against steel and sapphire surfaces. The measured temperatures were compared with flash temperature predictions. The role of transfer films were discussed.

2. Materials and methods

PEEK balls were rubbed against steel and sapphire discs in a ball-on-disc configuration. Friction and interfacial temperatures were recorded at various sliding speeds and applied loads. Both steel and sapphire discs were used for friction measurements while only sapphire discs were used for IR thermography temperature measurements.

2.1. Materials

PEEK ball samples were made from a commercially available Victrex 450G injection molded bar stock. The 19 mm diameter balls were machined from a single 25 mm diameter rod on a 3-axis CNC lathe to ensure reproducibility between samples. Steel and sapphire discs for friction measurements were purchased from PCS. The material properties of the balls and discs are listed in Table 1. Contacts were formed when a PEEK ball was pressed against a disc. The ball was always stationary while the disc rotated at a programmed speed. The labeling PEEK-sapphire and PEEK-steel denote contacts formed with a PEEK ball, against a sapphire disc and a steel disc respectively.

2.2. Friction measurement

Coefficients of friction were measured using a mini-traction machine (MTM) from PCS instrument under pure sliding conditions [51]. Tests were done by pressing a 19 mm diameter PEEK ball on a rotating disc. A new disc specimen was used for each test. Discs were cleaned with toluene in an ultrasonic bath and washed with acetone before use. PEEK balls were rinsed in isopropanol and thoroughly dried before each test. All tests were conducted at 25 °C.

In this study, the effects of speed and load on friction coefficient were investigated. Friction was measured across a range of loads between 1 N and 40 N at a fixed sliding speed of 100 mm/s. The

Table 1
Material properties of balls and disc substrates.

Material (source)	Dimensions (mm diameter)	Hardness	Roughness, *Ra* (nm)
PEEK balls (Victrex 450G)	19	84.5 Shore-D	1500
MTM Steel AISI 52100 disc (PCS)	46	760 HV	<10
MTM Sapphire disc (PCS) (for friction measurements)	46	2000 HV	<20
Sapphire disc (for temperature measurements)	100	2000 HV	7

change in friction as a function of sliding speed was also measured at a fixed load of 10 N over sliding speed range of 1–4000 mm/s. Friction was reported as the average of five data points taken at the desired load and speed. Each data point represents approximately a 5-s period of sliding. The duration of sliding was 12 min for fixed load, increasing speed tests and 3 min for fixed speed, increasing load tests. All tests were repeated at least twice.

2.3. Temperature measurement

The surface temperature of a rubbing contact, T_s, was examined with IR thermography for PEEK-sapphire contacts. Details of the setup and calibration procedures are described in Ref. [21]. Briefly, the rubbing contact was created with an EHL rig (manufactured by PCS instrument), where a stationary PEEK ball was pressed against a rotating sapphire disc from the bottom, as shown in Fig. 1. A sapphire disc, which fully transmits infrared radiation in the wavelength range of 3–5 μm, was used as the counterface. As the contact heated up, infrared (IR) radiation was emitted. An infrared camera X6540SC (FLIR), placed above the contact, detected the IR radiation emitted from the contact (see Fig. 1). The camera had a 320 × 256 focal plane array with a 5 × lens and 6.3 μm resolution. The observables are IR intensity images.

When a PEEK-sapphire contact was heated up, IR was emitted at the interface and the bulk sapphire disc. In order to detect T_s with IR thermography, calibrations are needed to remove the IR contribution from the bulk sapphire disc. The calibration was conducted using the same setup shown in Fig. 1 with a stationary contact formed by pressing a stationary PEEK ball against a stationary sapphire disc. The temperature of the contact was controlled by partially immersing the ball in a silicone oil bath at a predetermined temperature while the contact remained dry. A thermocouple was placed inside the PEEK ball just below the contact to estimate T_s. Once the estimated T_s from the thermocouple matched that of the oil bath, the IR signals detected by the camera were recorded. At a predetermined temperature, the calibration required collections of IR signals from two different sapphire discs, one normal (uncoated) sapphire disc and one coated with a thin layer of Aluminum on the contact surface. IR signals obtained with the uncoated sapphire disc, $C_{Uncoated}$, contain contributions from both the contact interface and the heated sapphire disc. Due to low IR emissivity of aluminium, the IR signals from the coated disc, C_{Al}, comes only from the heated disc. The IR signal from the contact is then $C_{Uncoated}-C_{Al}$. The interfacial temperature can be obtained using the relationship: $T_s = f(C_{Uncoated} - C_{Al})$. Calibration was performed for a temperature up to 110 °C and corresponding calibration curves shown in Figs. S1 and S2 in the supplementary data were used to create temperature maps with IR intensity images.

2.4. Orientation of transfer film

The orientation of transfer film was examined with Fourier transform infrared spectroscopy (FTIR, Shimadzu IRAffinity-1) using an ATR accessory (PIKE MIRacle). Measurements were taken using a ZnSe polarizer (Spectra-Tech) set parallel and perpendicular to the sliding direction. Backgrounds were taken with the polarizer in place. Only the polarizer was rotated between measurements. IRSolution software from Shimadzu was then used to remove the background from the measurements. The dichroic ratio D is the ratio of absorbance peaks from the parallel and perpendicular spectra $D = A_{\parallel}/A_{\perp}$. Large D signifies high dichroism due to chain alignment. Typically, D increases for increasing draw ratios λ but they are not equivalent.

3. Results and discussion

3.1. Effect of PEEK-countersurface interactions on PEEK friction

Friction measurements were performed with applied normal load W and sliding speed U as variables. Fig. 2A shows how the friction coefficients $\mu = F/W$, F being the frictional force, changes

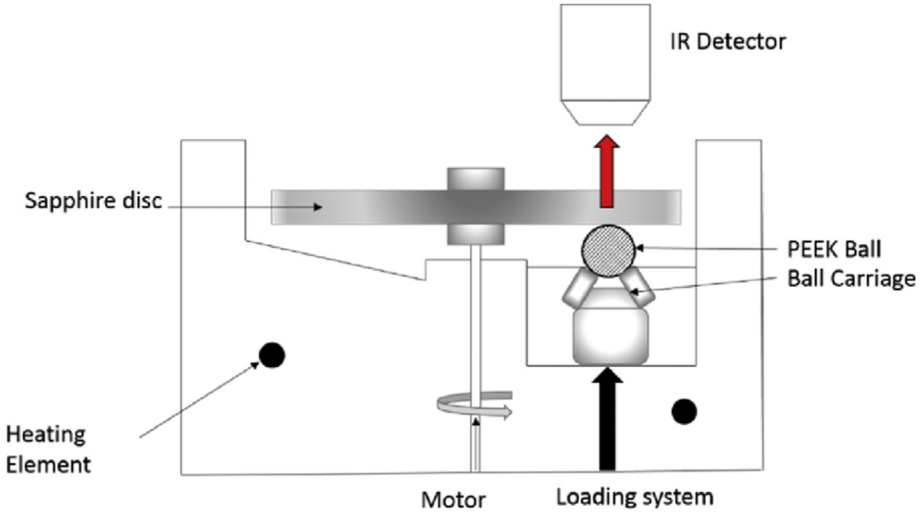


Fig. 1. Illustration of In-Situ IR measurement.

with load at a constant $U = 100$ mm/s. It shows that μ drops with increasing load. A power law fit gives $\mu = 0.33W^{-0.15}$ and $\mu = 0.5W^{-0.1}$ for PEEK-sapphire (circles, Fig. 2A) and PEEK-steel contacts (squares, Fig. 2A) respectively. This is inconsistent with Amonton's laws for friction with constant μ. Such inconsistency has been observed in polymers [52–55]. The relationship $\mu \propto W^{n-1}$ is governed by how the contact area changes with applied load W, i.e. the nature of the contact [35]. Results in Fig. 2A suggest that plastic deformation of asperities on rough surfaces dominates in our test conditions.

Note μ for PEEK-steel contacts are nearly twice that of PEEK-sapphire contacts (see Fig. 2A). Strongly adhered debris was found on the steel counterface (see Fig. S3 in supplementary information) but not on the sapphire surface after friction tests. Debris may form due to hard counterface asperities penetrating and cutting into the softer polymer surface. This can contribute to friction although it will not be significant due to both steel and sapphire counterfaces being smooth (R_a = 10–20 nm). Friction is also governed by both the elastic-plastic deformation and adhesion of sliding bodies [56,57]. Note the compressive yield strength of PEEK is approximately 125 MPa at ambient conditions [58,59]. For $W = 40$ N, the initial nominal and peak Hertzian contact pressures are about 76 MPa and 114 MPa respectively (see Section S.4 in supplementary information) for both contacts. Thus friction due to ball deformation for both contacts is likely to be similar. Both contacts result in PEEK ball wear scars of similar size (see Fig. S4 in supplementary information). Hence the contributions to friction due to increased true area in both contacts are likely to be comparable.

PEEK wear properties are linked to the chemical reactivity of the counterfaces [50–52]. During rubbing, adhesive transfer of debris, degradation of PEEK, and oxidation of the countersurface may all take place. Adhesive friction is influenced by the interactions between rubbing surfaces. Compared to steel, sapphire is both harder and more chemically inert. Indeed PEEK has been shown to be a suitable adhesive for bonding steel surfaces together [60]. Studies of the adhesive interface between PEEK and both 1010 carbon steel and 304 stainless steel created at 400 °C suggests the formation of Fe-O-C and Cr-O-C compounds [60,61]. Applied shear force during rubbing may allow their formations at more moderate temperatures and higher rate. This may explain the observation of a distinct red hue towards the edges of the PEEK ball wear scar formed when rubbed against steel (see white arrow in Fig. S4 in supplementary data). The red hue is believed to be iron oxide Fe_2O_3 that is transferred from the steel counterface. This together with the observation that well-adhered debris and transfer films are present only on steel counterface (see Fig. S3 in supplementary information) support that the interaction and interfacial strength, and hence adhesive friction is higher for PEEK-steel than that of PEEK-sapphire contacts. This can give rise to overall higher μ for PEEK-steel contacts observed in Fig. 2A.

3.2. Effect of sliding speed on PEEK friction

How friction coefficients of PEEK-steel and PEEK-sapphire contacts vary with sliding speed U at a constant load $W = 10$ N is presented in Fig. 2B. For PEEK-sapphire contact (circles in Fig. 2B), μ increases gradually with $U = 1$–50 mm/s. It then increases more rapidly until a maximum is reached and drops off around $U = 1$ m/s. Similar observations have been reported [5,62]. When U is low, frictional heat is not significant. However, the contact area changes as the result of local plastic deformation of surface asperities and increases with U. The contact area grows from partial to full contact, resulting in higher μ. At $U = 1$ m/s μ reaches a maximum then drops with U (circles in Fig. 2B). This transition is often attributed to thermally induced softening or melting and polymer friction enters the "thermal control regime" [5]. In this regime, the contact experiences significant frictional heating. The contact temperature may approach the glass transition temperature T_g of the polymer. As a result, polymer surface softens and thus slides more easily and friction rapidly drops with $\mu \propto 1/U$ [5]. The drop observed for PEEK-sapphire contacts in Fig. 2B seems more substantial although there are not enough data points above $U = 1$ m/s to make a conclusion.

For a PEEK-steel contact (squares in Fig. 2B), μ grows initially until $U \approx 10$ mm/s, after which it reaches a plateau. μ becomes more variable from $U \approx 1$ m/s but it is difficult to conclude if a transition has occurred based on Fig. 2B alone. The contact temperature in a PEEK-steel contact increases at the same time (details in section 3.3). These results are inconsistent with the thermal control model for friction [5]. In all cases, some well adhered debris is only found on steel counterfaces (Fig. S3C in supplementary information). These debris are likely to affect friction and surface temperatures of the contact and may explain the observed differences in μ between the PEEK-sapphire and PEEK-steel contacts.

3.3. The effects of load and sliding speed on contact temperature

Frictional heating can soften polymer surfaces and thus influence the effects of load and sliding speed on PEEK friction. To check if frictional heating was significant in our test conditions, IR thermography was applied to PEEK-sapphire contacts as outlined in section 2.3.

The contact temperature rise in PEEK-sapphire contact is denoted as $T_{sapphire}$. The corresponding estimated T_s is thus ($T_{sapphire}$ + 25 °C). For the variable load experiments conducted from $W = 2$–40 N at low sliding speed $U = 100$ mm/s (presented in

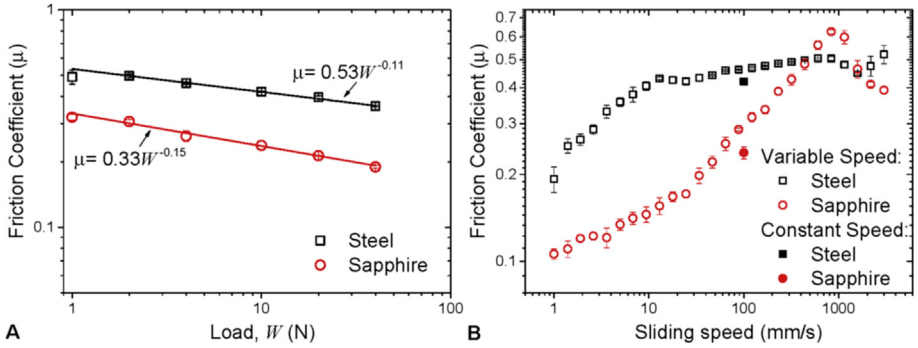


Fig. 2. Evolution of friction coefficient μ of PEEK ball against steel and sapphire discs: (A) with increasing load W and the sliding speeding U was 100 mm/s. The duration of each data point was 180 s; (B) with increasing U and constant W = 10 N. The duration of each test was 720 s (on average 40 s per data point).

Fig. 2A), a maximum $T_{sapphire}$ ~7 °C is observed (see Fig. 3). Note the contact area grows with increasing normal load. The contact area is made of patches at low loads. With increasing load, partial contact develops into full contact (see Fig. 3). These observations suggest that results in Fig. 2A are in load controlled friction regime and thermal effect is not important when sliding speed is low. Since similar relationships between μ and W were observed for both PEEK-steel and PEEK-sapphire contacts, it is likely that thermal effect is insignificant in both contacts under these low sliding speed conditions.

The temperature maps generated with IR thermography for PEEK-sapphire contacts with $W = 10$ N at various U from 100 mm/s to 4 m/s are shown in Fig. 4 (see Fig. S2B in supplementary information for corresponding temperature profiles). For $U = 100$–200 mm/s, only slight temperature rise is observed. As U increases, the contact shape changes significantly and $T_{sapphire}$ increases. Assuming that the real area of contact A_r corresponds to the hottest sections of the temperature maps, both Fig. 4 and Fig. S2B show that A_r grows with speed until $U = 500$ mm/s. This was accompanied by a modest temperature rise. This supports that the initial increase of μ with U for PEEK-sapphire contact in Fig. 2B is due to an increase in A_r. For U above 500 mm/s, a distinct hot zone has been established, and $T_{sapphire}$ increases further. For U above 1 m/s, $T_{sapphire}$ of 45 °C is observed, giving a maximum T_s ~70 °C. This is however below T_g of PEEK ~150 °C. Thus the contact temperature alone may be insufficient to soften PEEK.

For U above 1 m/s significant heat drag was observed in Fig. 4 (see also Fig. S2B in supplementary data). This phenomenon is common for conditions with large Peclet numbers Pe [20]. $Pe = 2Ua/\chi$ where a and χ are radius of the contact and thermal diffusivity of the disc respectively. It governs the resulting temperature distribution in the disc. The heat partition between the disc and the ball is described by the heat partition coefficient α. Laraqi has analytically shown that for $Pe > 20$ considerable heat drag develops [20]. There also appears to be a threshold velocity where $Pe > 30$ and α no longer changes [20]. Since the sapphire disc has a higher thermal conductivity than the PEEK ball, the portion of the frictional heat conducted into the moving sapphire disc $\alpha_{disc} > 0.97$ for all U tested (see Section S.6 in supplementary information). Unless heat generated at the contact is removed at a sufficiently fast rate by the highly conductive disc, the surface temperature will rise with increased sliding [19]. For the experimental conditions used in this study Pe ~ 20 at 1.08 m/s and 30 at 1.62 m/s. The observation of heat drag in Fig. 4 is similar to the response predicted by Laraqi [20] and observed by Rowe [19]. The amount of retained heat at a specific disc location will depend on the duration for heat conduction between two subsequent contacts with the PEEK ball. Note the sapphire discs for friction tests (Fig. 2) and IR thermography (Fig. 4) were 46 mm and 100 mm respectively. Keeping U constant, the smaller disc for friction tests would allow less time for heat removal. Hence higher T_s may occur during friction measurements as compared to 70 °C seen in IR thermography. A higher T_s may give rise to a drop in μ with U at high U.

Since steel is not IR transparent, a thermocouple was used to detect the counterface temperature rise just behind the trailing edge of the PEEK-steel contact T_{steel} with $W = 10$ N and sliding speeds $U = 10$ mm/s, 100 mm/s, 2 m/s and 4 m/s. Note T_{steel} is likely to be lower than the actual temperature rise in the contact. How μ and T_{steel} change with time are shown in Fig. 5. At $U = 10$ and 100 mm/s, μ grows within the first few seconds after which a constant μ is reached. This is accompanied by negligible T_{steel} for the duration of sliding (see Fig. 5B). However, at $U = 2$ and 4 m/s, μ fluctuates while T_{steel} increases quickly for about 180 s after which the increase slows down. The plateau μ ~ 0.5–0.6 in all conditions match relatively well with results shown in Fig. 2B (open squares).

T_{steel} is above 110 °C (i.e. T_s ~ 130 °C) after 300 s for $U = 4$ m/s. In these conditions, local contact temperature may approach PEEK's T_g ~150 °C. This together with results in Fig. 2B suggest that high contact temperature at a PEEK-steel contact with high U gives rise to a transition from stable to fluctuating μ. As will be shown in section 3.5, PEEK chains that made up the transfer film are highly aligned, suggesting that strain hardening effect of transfer film as sliding speed increases may be responsible for such transition. Thus thermal control model does not apply to PEEK-steel contacts within the conditions tested.

3.4. Comparison between predicted and measured contact temperature

Frictional heat generated at a contact impacts the coefficient of friction of the sliding contact. Ideally, contact temperatures should be measured *in situ*. However this may not be possible as in the case of PEEK-steel contacts. One can use various models to predict temperature rise. In this section, the validity of predicting contact temperature with the Jaeger's model is investigated. Details on flash temperature and pressure predictions, and relevant materials properties can be found sections S.4 and S.6 of the supplementary information.

Average flash temperature rise in a contact can be estimated using Jaeger's solution assuming a uniform circular source [16] or with other models such as that by Tian and Kennedy [17] or Archard [12]. Rowe et al. derived a partitioned flash temperature solution for a moving heat source based on these models and an equation based on Jaeger's model is used for the predicted temperature rise [19]. The heat flux density $\dot{q}$ due to friction μ is $\dot{q} = \mu pU$ where p is the average normal pressure and U the sliding speed. Predictions can be made assuming the pressure is Hertzian and constant. Fig. 6 shows predictions of flash temperatures T_f of a PEEK ball against sapphire $T_f(sapphire)$, steel $T_f(steel)$, and PEEK $T_f(PEEK)$ at various speeds and $W = 10$ N based on nominal pressure (average pressure $P_{ave} = 48$ MPa). $T_f(sapphire)$ and $T_f(steel)$ are based on measured μ (see Fig. 2B) and $T_f(PEEK)$ with $\mu = 0.3$ [63]. The average flash temperature for the PEEK-sapphire contact $T_{sapphire-ave}$ is obtained by IR temperature maps shown in Fig. 4 and is compared to $T_f(sapphire)$ in Fig. 6. $T_{sapphire-ave}$ (solid squares, Fig. 6) and the prediction $T_f(sapphire)$ (open squares, Fig. 6) follow a similar functional form. They match relatively well. This gives confidence to the

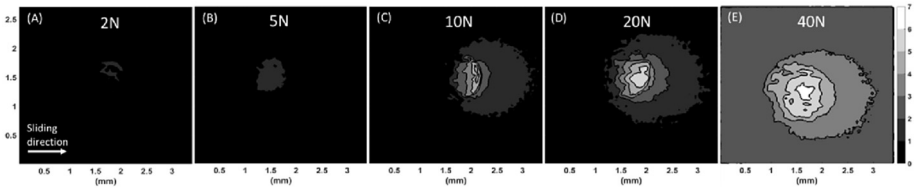


Fig. 3. Maps of surface temperature rise $T_{sapphire}$ at constant speed U = 100 mm/s and increasing load W for stationary PEEK ball against sliding sapphire counterface. Each image corresponds to the temperature at time = 5 min. The grey scale shows the local temperature rise (°C) in the contact.

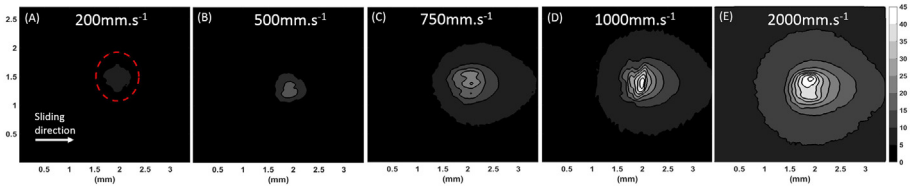


Fig. 4. Surface temperature rise $T_{sapphire}$ for constant load $W = 10$ N and increasing speed U for stationary PEEK ball against sliding sapphire counterface. Each image was taken at time = 5 min. The grey scale shows the local temperature rise (°C) in the contact.

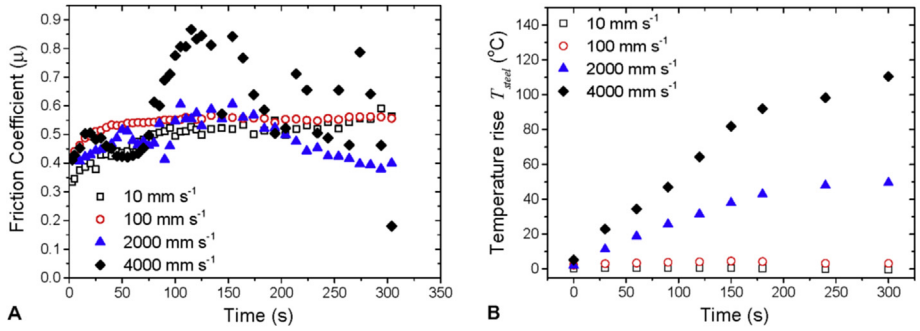


Fig. 5. Evolution of (A) coefficient of friction μ and (B) counterface temperature T_{steel} over time for stationary PEEK ball against sliding steel counterface. $W = 10$ N. Each tests lasted 5 min. Data were captured every 100 s.

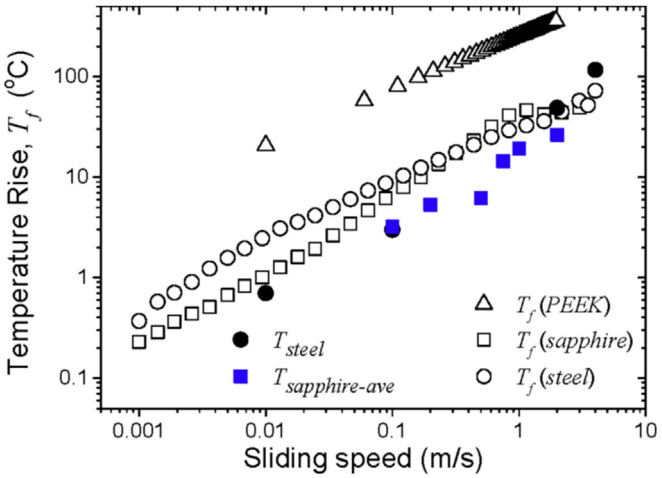


Fig. 6. Comparison between flash temperatures predictions and measurements. All open symbols are predictions on flash temperatures T_f based on average pressure for stationary PEEK ball against rotating PEEK, sapphires, and steel discs at W = 10 N. Actual μ is taken from Fig. 2B; Solid symbols are experimental results with $T_{sapphire-ave}$ being average $T_{sapphire}$ for IR thermography in PEEK-sapphire contacts, and T_{steel} being temperature at the trailing edge of the PEEK-steel contacts.

use of these flash temperature prediction models for PEEK contacts. $T_{sapphire-ave}$ is slightly lower than $T_f(sapphire)$. This maybe because PEEK balls wears quickly during experiments as such contact area increases and pressure decreases quickly, resulting in lower than expected temperature rise. Note higher temperatures may occur locally at asperities before this steady state is reached. Such temperature spikes, if they exist, appear to be on a time and spatial scale smaller than the resolutions of the IR camera (500 μs and 20 μm respectively).

The thermal conductivity of the counterface plays a significant role in determining T_f. Steel and sapphire are good thermal conductors. They have similar thermal conductivity K and diffusivity χ. Hence $T_f(sapphire)$ and $T_f(steel)$ are similar (see open squares and open circles in Fig. 6). PEEK is a good thermal insulator and much softer than any of the other counterfaces. Its low K and χ as well as larger Hertzian contact area thus lead to high $T_f(PEEK)$ (open triangles, Fig. 6). Note, while the predicted $T_f(PEEK)$ is higher than PEEK T_g when $U > 0.2$ m/s, in practice the contact temperature will be capped at the softening temperature of the PEEK until sufficient latent heat is absorbed.

Compare $T_f(steel)$ and T_{steel}, they match well up to $U = 1$ m/s (circles, Fig. 6). T_{steel} and $T_{sapphire-ave}$ were also similar in this speed range. At $U = 4$ m/s, $T_f(steel)$ is slower than T_{steel}. This can be due to an increase of average disc temperature as heat built up. Note that well-adhered debris and transfer films found on steel counterfaces (see Fig. S3 in supplementary information) could create local PEEK-PEEK contacts. As $T_f(PEEK)$ is higher than $T_f(steel)$, these local PEEK-PEEK contacts may result in higher overall temperatures than that of PEEK-bare steel contact. T_{steel} is however below $T_f(PEEK)$ because the transfer films are patchy. Thus the PEEK ball is in contact with both patchy transfer film and bare steel (see Figs. S3 C and D). This shows that the existence of transfer films, especially one with incomplete coverage of the counterface, may render the flash temperature prediction inaccurate.

3.5. The nature of transfer films and their role on friction mechanisms

PEEK debris are found for both PEEK-steel and PEEK-sapphire contacts. In the case of PEEK-steel contacts, transfer films are formed. Both PEEK debris and transfer films can affect contact temperature and friction. Debris forms as the subsurface shear stress surpasses bulk shear yield stress. If the adhesion between PEEK and counterface is strong, PEEK debris may adhere on the counterface. This is the case for PEEK-steel interface. The localized PEEK-PEEK contacts created within the PEEK-steel contact may promote frictional heating. The temperature of these localized PEEK-PEEK contacts may reach T_g ~150 °C with modest sliding speeds and the melting point T_m ~350 °C at U ~2 m/s (see $T_f(PEEK)$ in Fig. 6). Thin PEEK films can then form potentially by shearing of

debris under localized heating. Indeed patches of transfer films are found on steel counterfaces. They consist of long thin sections of films (see Fig. S3) and adhere to the surface strongly. Some sections have roughly uniform thickness (~1 μm thick). Thicker fragments (white arrows in Fig. S3) roughly 3–5 μm thick are also found. They exist in all test conditions with PEEK-steel contacts but are most prevalent for $U \geq 2$ m/s. This may explain the observed μ fluctuations at high sliding speed for PEEK-steel contacts (Fig. 5A). This is similar to the PTFE delamination phenomenon in relationship with sliding conditions as described by Blanchett [64]. Low wear and friction correspond to drawing of fibrils across the sliding surface. However, severe wear was due to subsurface deformation, fracture and debris formations. It is suggested that this transition from fibril drawing to delamination depends on how friction changes with temperature and sliding speed.

A polymer's ability to form thin continuous transfer layers is related to its drawability [57]. PEEK can undergo large deformations before break (draw ratios λ ~3) at temperatures above T_g and can be drawn into highly oriented films [65–67]. Infrared dichroic ratio of a film can be used to assess the degree of chains orientation of a film and have been applied to PEEK [68,69]. Note large dichroic ratio D signifies high dichroism due to chain alignment. While dichroic ratio D increases with increasing draw ratios λ, they are not equivalent. Transfer films formed on a steel counterface during constant load friction experiment (Fig. 2B) were carefully removed and was examined with ATR-FTIR (see section 2.4). The resulting spectra are shown in Fig. 7. They show similarly high dichroism at all wavenumbers κ. The diphenyl ether peak at $\kappa = 1190$ cm^{-1} gives $D = 3.4$ and the $\kappa = 1648$ cm^{-1} band associated with stretching of carbonyl groups gives $D = 2.8$. These results support the transfer films are highly stretched and chains are aligned in the direction of sliding. Measurements were also taken of the wear scar and untested sections of the ball. Neither surface shows evidences of chain orientation. The ball wear surface may exhibit some orientation but the underlying bulk material masks the signal. Further work to understand film structure and any possible molecular orientation will be needed.

The high dichroic ratio of transfer films is intriguing. Subsurface delamination, as well as surface melting can both be responsible for surface deposition. Note PEEK deposition occurs on steel counterface even at $U = 100$ mm/s, where difference in contact and ambient temperature is negligible. The contact temperature reaches 130 °C only around $U = 4$ m/s. The amount of deposits (including transfer film) increased with U. This suggests that high temperature may not be necessary for the initial PEEK deposition on steel. However the initial deposits give rise to local frictional heating which may further promote more deposits and drawing of transfer layers.

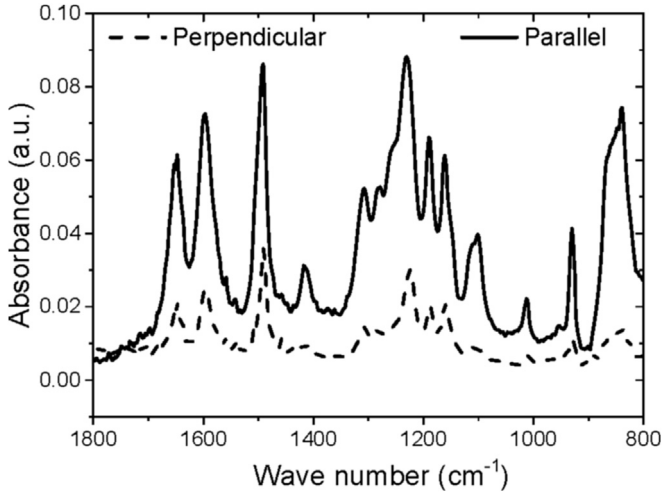


Fig. 7. Polarized FTIR-ATR measurement of transfer film parallel and perpendicular to sliding direction.

4. Conclusion

In this study, the tribology of PEEK was monitored under dry sliding conditions with pressure and velocity as variables. Stainless steel (AISI 52100) and sapphire counterfaces were used. They had similar roughness (R_a = 10–20 nm) but resulted in very different friction behavior. PEEK-steel contacts have greater adhesive friction than PEEK-sapphire contacts. Under all test conditions, PEEK debris is found adhered to the steel surface. Iron oxide residue also appears on the PEEK wear scars. The transfer of debris to the surface explains how local temperatures may approach T_g.

Average temperature rise for both PEEK-sapphire and PEEK steel contacts were predicted and compared with measured temperature rise. The measured temperatures match reasonably well with predicted results with the former slightly lower than the latter. This is due to wear of PEEK balls reducing the actual pressure and hence temperature at the contact. For PEEK-steel contacts, flash temperature prediction at high speed is lower than measured contact temperature. Well adhered deposits may give rise to the localized heating and promote transfer film formations. The failure to take into account the existence of transfer film may be responsible for under prediction of surface temperature for PEEK-steel contact. The PEEK transfer film on steel counterface is highly oriented which suggests its formation process is similar to drawing or extrusion of polymers at high temperature. While the observed temperature rise suggests that drawing and chain alignment of PEEK can occur at lower temperature, the possibility of localized heating between PEEK deposit and PEEK ball cannot be ignored. The friction and surface temperatures for PEEK depend on this transfer film formation process and cannot be explained by pressure and velocity alone.

Acknowledgement

KAL is supported by Advanced Polymers for Energy Applications (APPEAL) consortium at Texas A&M University. AJF is supported by Hoerbiger UK Limited and EPSRC. HJS is partially supported by the Ocean Energy Safety Institute (OESI). OESI is funded under the award (E14AC00001) that is granted by the Bureau of Safety and Environmental Enforcement (BSEE) of the U.S. Department of the Interior. The authors gratefully acknowledge Dr Tom Reddyhoff for the use of his IR thermography setup; and Drs Amir Kadiric, Marc Masen and Luca di Mare for very fruitful discussions.

Appendix A. Supplementary data

Supplementary data related to this article can be found at http://dx.doi.org/10.1016/j.polymer.2016.09.064.

References

[1] J. Dyson, W. Hirst, The true contact area between solids, Proc. Phys. Soc. Sect. B 67 (4) (1954) 309.
[2] C.W. McCutchen, Optical systems for observing surface topography by frustrated total internal reflection and by interference, Rev. Sci. Instrum. 35 (10) (1964) 1340–1345.
[3] P.W. O'Callaghan, S.D. Probert, Prediction and measurement of true areas of contact between solids, Wear 120 (1) (1987) 29–49.
[4] H. Blok, The flash temperature concept, Wear 6 (6) (1963) 483–494.
[5] C.M. McC. Ettles, Polymer and elastomer friction in the thermal control regime, ASLE Trans. 30 (2) (1987) 149–159.

[6] K.G. Plumlee, C.J. Schwartz, Surface layer plastic deformation as a mechanism for UHMWPE wear, and its role in debris size, Wear 301 (1–2) (2013) 257–263.
[7] K.A. Laux, C.J. Schwartz, Influence of linear reciprocating and multi-directional sliding on PEEK wear performance and transfer film formation, Wear 301 (1–2) (2013) 727–734.
[8] G. Zhang, A.K. Schlarb, Correlation of the tribological behaviors with the mechanical properties of poly-ether-ether-ketones (PEEKs) with different molecular weights and their fiber filled composites, Wear 266 (1) (2009) 337–344.
[9] M.Q. Zhang, et al., Frictional surface temperature determination of high-temperature-resistant semicrystalline polymers by using their double melting features, J. Appl. Polym. Sci. 63 (5) (1997) 589–593.
[10] K.A. Laux, et al., Wear behavior of polyaryletherketones under multi-directional sliding and fretting conditions, Tribol. Lett. 58 (3) (2015) 1–13.
[11] S.H. Rhee, K.C. Ludema, Mechanisms of formation of polymeric transfer films, Wear 46 (1) (1978) 231–240.
[12] J.F. Archard, The temperature of rubbing surfaces, wear 2 (6) (1959) 438–455.
[13] K. Tanaka, Y. Uchiyama, Friction, wear and surface melting of crystalline polymers, in: Abstracts of Papers of the American Chemical Society, Amer Chemical Soc, 1155 16TH ST, NW, Washington, DC 20036, 1974.
[14] G. Stachowiak, A.W. Batchelor, Engineering Tribology, Butterworth-Heinemann, 2013.
[15] J.F. Archard, R.A. Rowntree, The temperature of rubbing bodies; part 2, the distribution of temperatures, Wear 128 (1) (1988) 1–17.
[16] J.C. Jaeger, Moving sources of heat and the temperature of sliding contacts, J. Proc. R. Soc. N. S. W. 76 (1942) 203–224.
[17] X. Tian, F.E. Kennedy, Maximum and average flash temperatures in sliding contacts, J. Tribol. 116 (1) (1994) 167–174.
[18] F.E. Kennedy, Frictional heating and contact temperatures, Mod. Tribol. Handb. 1 (2001) 235–259.
[19] K.G. Rowe, et al., In situ thermal measurements of sliding contacts, Tribol. Int. 62 (2013) 208–214.
[20] N. Laraqi, et al., Temperature and division of heat in a pin-on-disc frictional device—exact analytical solution, Wear 266 (7) (2009) 765–770.
[21] J. Le Rouzic, T. Reddyhoff, Development of infrared microscopy for measuring asperity contact temperatures, J. Tribol. 135 (2) (2013) 021504.
[22] A.I. Bennett, K.G. Rowe, W.G. Sawyer, Dynamic in situ measurements of frictional heating on an isolated surface protrusion, Tribol. Lett. 55 (1) (2014) 205–210.
[23] C. Putignano, et al., A theoretical and experimental study of viscoelastic rolling contacts incorporating thermal effects, Proc. Institution Mech. Eng. Part J J. Eng. Tribol. 228 (10) (2014) 1112–1121.
[24] G. Fortunato, et al., General theory of frictional heating with application to rubber friction, J. Phys. Condens. Matter 27 (17) (2015) 175008.
[25] G.S. Underwood, Wear Performance of Ultra-performance Engineering Polymers at High PVs, 2002 (SAE Technical Paper).
[26] D. Kemmish, Update on the Technology and Applications of Polyaryletherketones, ISmithers, 2010.
[27] M.H. Mohammed, et al., Physical properties of poly (ether ether ketone) exposed to simulated severe oilfield service conditions, Polym. Degrad. Stab. 98 (6) (2013) 1264–1270.
[28] S.M. Kurtz, J.N. Devine, PEEK biomaterials in trauma, orthopedic, and spinal implants, Biomaterials 28 (32) (2007) 4845–4869.
[29] R.A. Rowntree, M.J. Todd, A review of European trends in space tribology and its application to spacecraft mechanism design, in: MRS Proceedings, Cambridge Univ Press, 1988.
[30] P.M. Dickens, J.L. Sullivan, J.K. Lancaster, Speed effects on the dry and lubricated wear of polymers, Wear 112 (3) (1986) 273–289.
[31] D.L. Burris, W.G. Sawyer, Hierarchically constructed metal foam/polymer composite for high thermal conductivity, Wear 264 (3) (2008) 374–380.
[32] J. Bijwe, S. Sen, A. Ghosh, Influence of PTFE content in PEEK–PTFE blends on mechanical properties and tribo-performance in various wear modes, Wear 258 (10) (2005) 1536–1542.
[33] G. Zhang, et al., Effects of sliding velocity and applied load on the tribological mechanism of amorphous poly-ether–ether–ketone (PEEK), Tribol. Int. 41 (2) (2008) 79–86.
[34] M.Q. Zhang, Z.P. Lu, K. Friedrich, On the wear debris of polyetheretherketone: fractal dimensions in relation to wear mechanisms, Tribol. Int. 30 (2) (1997) 87–102.
[35] Z.P. Lu, K. Friedrich, On sliding friction and wear of PEEK and its composites, Wear 181–183 (1995) 624–631. Part 2.
[36] T.A. Stolarski, Tribology of polyetheretherketone, Wear 158 (1) (1992) 71–78.
[37] T.C. Ovaert, H.S. Cheng, The unlubricated sliding wear behavior of polyetheretherketone against smooth mild-steel counterfaces, J. Tribol. 113 (1) (1991) 150–157.
[38] B.H. Stuart, Tribological studies of poly (ether ether ketone) blends, Tribol. Int. 31 (11) (1998) 647–651.
[39] D.L. Burris, W.G. Sawyer, A low friction and ultra low wear rate PEEK/PTFE composite, Wear 261 (3) (2006) 410–418.
[40] D.L. Burris, et al., Polymeric nanocomposites for tribological applications, Macromol. Mater. Eng. 292 (4) (2007) 387–402.
[41] C.M. Pooley, D. Tabor, Friction and molecular structure: the behaviour of some thermoplastics, Proc. R. Soc. Lond. Ser. A, Math. Phys. Sci. (1972) 251–274.
[42] S. Bahadur, The development of transfer layers and their role in polymer tribology, Wear 245 (1–2) (2000) 92–99.
[43] M.Q. Zhang, Z.P. Lu, K. Friedrich, Thermal analysis of the wear debris of polyetheretherketone, Tribol. Int. 30 (2) (1997) 103–111.
[44] T.Q. Li, et al., Friction induced mechanochemical and mechanophysical changes in high performance semicrystalline polymer, Polymer 40 (16) (1999) 4451–4458.
[45] Q. Zhao, S. Bahadur, The mechanism of filler action and the criterion of filler selection for reducing wear, Wear 225 (1999) 660–668.
[46] S. Bahadur, D. Gong, The action of fillers in the modification of the tribological behavior of polymers, Wear 158 (1) (1992) 41–59.
[47] S. Bahadur, D. Gong, J.W. Anderegg, The investigation of the action of fillers by XPS studies of the transfer films of PEEK and its composites containing CuS and CuF 2, Wear 160 (1) (1993) 131–138.
[48] O. Jacobs, et al., On the effect of counterface material and aqueous environment on the sliding wear of various PEEK compounds, Tribol. Lett. 18 (3) (2005) 359–372.
[49] O. Jacobs, et al., On the effect of counterface material and aqueous environment on the sliding wear of carbon fibre reinforced polyetheretherketone (PEEK), Tribol. Lett. 19 (4) (2005) 319–329.
[50] M. Rebelo de Figueiredo, et al., Adhesion tendency of polymers to hard coatings, Int. Polym. Process. 28 (4) (2013) 415–420.
[51] P.C.S. Instruments, MTM (Mini Traction Machine), 2016.
[52] S. Bahadur, Dependence of polymer sliding friction on normal load and contact pressure, Wear 29 (3) (1974) 323–336.
[53] J.F. Archard, Elastic deformation and the laws of friction, in: Proceedings of the Royal Society of London a: Mathematical, Physical and Engineering Sciences, The Royal Society, 1957.
[54] R.C. Bowers, Coefficient of friction of high polymers as a function of pressure, J. Appl. Phys. 42 (12) (1971) 4961–4970.
[55] V. Quaglini, P. Dubini, Friction of polymers sliding on smooth surfaces, Adv. Tribol. (2011) 2011.
[56] N.K. Myshkin, M.I. Petrokovets, A.V. Kovalev, Tribology of polymers: adhesion, friction, wear, and mass-transfer, Tribol. Int. 38 (11) (2006) 910–921.
[57] B.J. Briscoe, D. Tabor, Friction and wear of polymers: the role of mechanical properties, Br. Polym. J. 10 (1) (1978) 74–78.
[58] D.P. Jones, D.C. Leach, D.R. Moore, Mechanical properties of poly (ether-ether-ketone) for engineering applications, Polymer 26 (9) (1985) 1385–1393.
[59] Victrex PEEK™ 450G datasheet. Victrex Ltd. Available from: http://www.victrex.com/en/peek-450g-polymer.php.
[60] T. Sugama, N.R. Carciello, M. Miura, Adhesion of crystalline polyphenyletheretherketone (PEEK) in metal-to-metal joints, Int. J. adhesion adhesives 12 (1) (1992) 27–37.
[61] T. Sugama, N.R. Carciello, Polyphenyletherketone and polyphenylethersulfone adhesives for metal-to-metal joints, Int. J. Adhesion Adhesives 13 (4) (1993) 257–266.
[62] M. Watanabe, H. Yamaguchi, The friction and wear properties of nylon, Wear 110 (3) (1986) 379–388.
[63] Y. Yamamoto, T. Takashima, Friction and wear of water lubricated PEEK and PPS sliding contacts, Wear 253 (7–8) (2002) 820–826.
[64] T.A. Blanchet, F.E. Kennedy, Sliding wear mechanism of polytetrafluoroethylene (PTFE) and PTFE composites, Wear 153 (1) (1992) 229–243.
[65] V. Bassigny, et al., Tensile drawing of poly (aryl ether ether ketone): 1. birefringence, infra-red dichroism and shrinkage-stress measurements, Polymer 34 (19) (1993) 4052–4059.
[66] L.H. Lee, J.J. Vanselow, N.S. Schneider, Effects of mechanical drawing on the structure and properties of PEEK, Polym. Eng. Sci. 28 (3) (1988) 181–187.
[67] Y. Lee, J.M. Lefebvre, R.S. Porter, Uniaxial draw of poly (aryl-ether-ether-ketone) by solid-state extrusion, J. Polym. Sci. Part B Polym. Phys. 26 (4) (1988) 795–805.
[68] H.B. Daly, et al., An experimental technique for the characterization of molecular orientation through the thickness of plastic products, Polym. Eng. Sci. 39 (10) (1999) 1982–1992.
[69] P. Damman, et al., Liquid-liquid phase separation and oriented growth of poly (aryl ether ether ketone) on friction-transferred poly (tetrafluoroethylene) substrates, Macromolecules 28 (24) (1995) 8272–8276.